Optics Letters

Simultaneous wideband radio-frequency self-interference cancellation and frequency downconversion for in-band full-duplex radio-over-fiber systems

YANG CHEN[1,3,*] AND SHILONG PAN[2]

[1]Shanghai Key Laboratory of Multidimensional Information Processing, East China Normal University, Shanghai 200241, China
[2]Key Laboratory of Radar Imaging and Microwave Photonics, Ministry of Education, Nanjing University of Aeronautics and Astronautics, Nanjing 210016, China
[3]School of Information Science and Technology, East China Normal University, Shanghai 200241, China
*Corresponding author: ychen@ce.ecnu.edu.cn

Received 17 April 2018; revised 25 May 2018; accepted 26 May 2018; posted 1 June 2018 (Doc. ID 327641); published 25 June 2018

A photonic approach for simultaneous wideband radio-frequency (RF) self-interference cancellation and frequency downconversion in an in-band full-duplex radio-over-fiber system is proposed based on a dual-polarization quadrature phase-shift keying (DP-QPSK) modulator. The upper dual-parallel Mach–Zehnder modulator (DP-MZM) in the DP-QPSK modulator is used to cancel the self-interference directly in the optical domain and generate two sidebands of the desired RF signal, whereas the lower DP-MZM generates two sidebands of the local oscillator. After detecting the combined optical signal at a photodetector, the desired RF signal is downconverted to an intermediate frequency (IF) signal with the self-interference cancelled. The proposed approach can overcome the reappearance of the interference signal and the power fading effect of the received signal caused by fiber dispersion. An experiment is performed. The cancellation depth for single frequency interference cancellation is around 58 dB, whereas that for the wideband interference cancellation is larger than 25 dB. The fading effect of the proposed IF transmission system is also evaluated compared with the traditional RF transmission system.

OCIS codes: (060.5625) Radio frequency photonics; (060.2360) Fiber optics links and subsystems; (070.1170) Analog optical signal processing; (350.4010) Microwaves.

https://doi.org/10.1364/OL.43.003124

Radio-over-fiber (ROF) systems, which are an integration of wireless and optical systems, have attracted great attention during the past few years and are considered to be a promising solution to increase the bandwidth, capacity, and mobility for both mobile and fixed users [1]. Conventionally, the frequencies of the uplink and downlink of an ROF system are different to avoid interference. However, the limited spectral resources and the ever-increasing demand for higher data rates have motivated the new in-band full-duplex ROF systems, where the frequencies of uplink and downlink are identical to improve the throughput and spectrum efficiency [2].

The main challenge faced in the in-band full-duplex ROF system is self-interference, which is difficult to eliminate by simply using an electrical filter because of the in-band operation. Many efforts have been made to eliminate the self-interference in the electrical domain [3,4]. The main limitation of the electrical self-interference cancellation (SIC) method is that its operating bandwidth and frequency are limited due to the well-known electronic bottleneck. In order to solve the limitations encountered in the electrical SIC systems, photonic-assisted SIC systems have been widely studied in recent years, taking advantage of the low loss and wide bandwidth offered by modern photonics [5]. In [6,7], radio-frequency (RF) SIC is achieved by using two parallel Mach–Zehnder modulators (MZMs) biased at opposite quadrature transmission points. In [8], another approach is demonstrated, using two electro-absorption modulators (EAMs) and a balanced photodetector (BPD) for interference subtraction. Similar structures using two electro-absorption modulated lasers instead of the laser and EAMs used [8] are proposed in [9]. In addition, the signal subtraction is realized by inverting the interference signal directly in the electrical domain in the transmitter in [9], so that the BPD used in [8] can be replaced by a single port photodetector (PD). In [10], parallel polarization modulators are used to realize RF SIC. The approaches demonstrated in [6–10] all employ two optical paths, which may make the system unstable during long-term operation. In [11,12], RF SIC systems based on a single modulator are proposed.

In the approaches in [6–12], the self-interferences are cancelled in the electrical domain after photodetection. It is well known that the received signals in the base stations are sent back to the central office via optical fibers. When the frequency of the signal is low (hundreds of MHz or several GHz), fiber dispersion can be ignored because the typical distance between

base stations and the central office is no more than 30 km. However, when the frequency of the received signal is very high, for example tens of GHz, the influence of fiber dispersion cannot be ignored. The dispersion induced by optical fibers will distort the phase relationship of the optical sidebands, which may influence the cancellation performance of the system. Furthermore, if the desired optical signal is the most commonly used double-sideband (DSB) modulated signal, fiber dispersion will also introduce the so-called fading effect, which may decrease the power of the desired RF signal [13]. For high frequency in-band full-duplex ROF systems, we believe there are two ways to eliminate or reduce the influence of fiber dispersions on the RF SIC systems: one is using some approach to compensate the dispersion induced distortion; the other is downconverting the signal to the intermediate frequency (IF) band while doing the RF SIC.

In this Letter, we propose a photonic approach for simultaneous wideband RF SIC and frequency downconversion based on a dual-polarization quadrature phase-shift keying (DP-QPSK) modulator. To the best of our knowledge, this is the first RF SIC system with simultaneous frequency downconversion. Using the proposed system, self-interference is cancelled directly in the optical domain, and high frequency received signals can be downconverted to IF signals simultaneously, so that the fiber dispersion induced in the transmission from the base station to the central office will not cause the cancellation performance degradation and the power fading of the desired RF signal. An experiment is performed. SIC in a wide frequency range is demonstrated both in single frequency and in wideband. The cancellation depth for single frequency SIC can be 58 dB, whereas that for the wideband SIC is larger than 25 dB.

Figure 1 shows the schematic diagram of the proposed system. A light wave generated from a laser diode (LD) is injected into a DP-QPSK modulator. The two RF ports of the upper dual-parallel MZM (DP-MZM) of the DP-QPSK modulator are driven by a corrupted signal ($A + B$) and a locally generated interference signal (B), where A is the desired uplink signal. One RF port of the lower DP-MZM is driven by the local oscillator (LO). The optical signal from the DP-QPSK modulator is sent to a polarizer via a polarization controller, where the two orthogonally polarized optical signals from the DP-QPSK modulator are 1:1 combined, which is then amplified by an erbium-doped fiber amplifier (EDFA) and detected in a PD.

The optical signal from DP-MZM1, whose two sub-MZMs are biased at the minimum transmission points (MITP) and main MZM is also biased at the MITP, can be expressed as

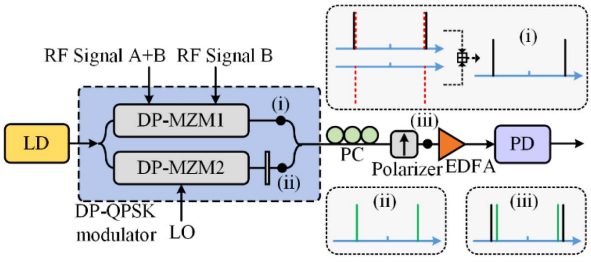

Fig. 1. Schematic diagram of the proposed RF SIC and downconversion system. LD, laser diode; DP-MZM, dual-parallel Mach–Zehnder modulator; PC, polarization controller; EDFA, erbium-doped fiber amplifier; PD, photodetector.

$$\begin{aligned} E_1(t) &\propto [\sin(\beta_1 \cos(\omega_s t + \varphi_1(t)) + \beta_2 \cos(\omega_s t + \varphi_2(t)))] \\ &\times \exp(j\omega_c t) + \sin(\beta_3 \cos(\omega_s t + \varphi_2(t))) \exp(j\omega_c t + j\pi) \\ &= [\sin(\beta_1 \cos(\omega_s t + \varphi_1(t)) + \beta_2 \cos(\omega_s t + \varphi_2(t))) \\ &- \sin(\beta_3 \cos(\omega_s t + \varphi_2(t)))] \exp(j\omega_c t), \end{aligned} \tag{1}$$

where ω_c is the angular frequency of the optical signal, ω_s is the angular frequency of the RF signal, V_π is the switching voltage of the modulator, $\beta_i = \pi V_i / V_\pi$ $(i = 1, 2, 3)$ is the modulation index, $V_i (i = 1, 2, 3)$ is the signal amplitude, and $\varphi_1(t)$ and $\varphi_2(t)$ are the information of the desired RF signal and the interference signal, respectively. Under specific conditions ($\beta_1 \ll 1$, $\beta_2 = \beta_3 \ll 1$), Eq. (1) is simplified as

$$E_1(t) \propto \beta_1 \cos(\omega_s t + \varphi_1(t)) \exp(j\omega_c t). \tag{2}$$

As can be seen from Eq. (2), the interference signal is cancelled in the optical domain, and a carrier-suppressed double-sideband (CS-DSB) optical signal carrying the desired RF signal is obtained. Actually, the condition for cancelling the interference can be more accurately expressed as $J_0(\beta_1)J_1(\beta_2) = J_1(\beta_3)$, when Eq. (1) is expanded and simplified using Jacobi–Anger expansions.

The two sub-MZMs in DP-MZM2 are biased at the MITP. ω_{LO} and β_{LO} are the angular frequency and the modulation index of the LO signal, respectively; $\beta_{\mathrm{LO}} = \pi V_{\mathrm{LO}} / V_\pi$; V_{LO} is the amplitude of the LO signal; β_x is the modulation index of the signal $V(t)$ applied to the other sub-MZM; and ϕ is the phase shift introduced by the main MZM. Here, $V(t) = 0$. Under the small signal modulation condition ($\beta_{\mathrm{LO}} \ll 1$), the optical signal from DP-MZM2 can be expressed as

$$\begin{aligned} E_2(t) &\propto \sin(\beta_x V(t)) \exp(j\omega_c t) \\ &+ \sin(\beta_{\mathrm{LO}} \cos \omega_{\mathrm{LO}} t) \exp(j\omega_c t + j\phi) \\ &\approx \beta_{\mathrm{LO}} \cos \omega_{\mathrm{LO}} t \exp(j\omega_c t + j\phi). \end{aligned} \tag{3}$$

The two orthogonally polarized optical signals from the two DP-MZMs are combined at the polarizer with its principle axis having an angle of 45 deg to one principle axis of the DP-QPSK modulator. The combined optical signal can be written as

$$\begin{aligned} E(t) &\propto \beta_1 \cos(\omega_s t + \varphi_1(t)) \exp(j\omega_c t) \\ &+ \beta_{\mathrm{LO}} \cos \omega_{\mathrm{LO}} t \exp(j\omega_c t + j\phi). \end{aligned} \tag{4}$$

After being detected at the PD with a responsivity of R, the photocurrent in the IF band can be expressed as

$$i(t) \propto R \cos \phi \beta_1 \beta_{\mathrm{LO}} \cos[(\omega_s - \omega_{\mathrm{LO}})t + \varphi_1(t)]. \tag{5}$$

It is observed that the desired RF signal at the IF frequency band is generated. To maximum the power of the downconverted IF signal, ϕ is set to 0. When fiber transmission is employed, it can be further deduced that the received IF power P can be expressed as

$$P \propto \cos^2(\pi D \lambda_c^2 L (f_s^2 - f_{\mathrm{LO}}^2)/c), \tag{6}$$

where D is the dispersion coefficient, λ_c is the central wavelength of the optical carrier, c is the speed of light in vacuum, L is the length of the optical fiber, f_s is the frequency of the RF signal, and f_{LO} is the frequency of the LO signal. When $f_{\mathrm{LO}} = 0$, that is, Eq. (4) is a DSB modulated signal, Eq. (6) degenerates to the equation of the power fading effect for the DSB modulated optical signal. It will be further proved by simulation that the fading effect for the IF signal caused by

fiber dispersion is small when the length of the fiber is shorter than 30 km and the frequency of the RF signal is less than 25 GHz.

An experiment based on the setup shown in Fig. 2 is carried out. A 16-dBm optical signal from a LD (Teraxion NLL) is sent to a DP-QPSK modulator (Fujitsu FTM7977), which has a 3 dB bandwidth of 23 GHz. The optical signal from the DP-QPSK modulator is sent to a polarizer via a PC. The combined optical signal from the polarizer is transmitted in a section of single-mode fiber (SMF), amplified by an EDFA (Amonics), and then detected in a PD (u2t) with about 40 GHz bandwidth. The interference RF signal is generated by an arbitrary waveform generator (AWG, Keysight M8195A), which is split into two paths by an electrical coupler (EC1). One part of the interference signal is combined with the desired RF signal, generated by a microwave signal source MSG1 (Agilent N5173B) via EC2 to simulate the received signal in in-band full-duplex ROF systems, which is applied to one RF port of DP-MZM1; the other part of the interference signal is sent to the other RF port of DP-MZM1. It should be noticed the amplitude and arrival time of the interference signals applied to the two sub-MZMs of DP-MZM1 need to have a fixed relationship, which is done by using an electrical delay line and an electrical attenuator. The LO signal is generated by MSG2 (AnaPico, APSIN20G), which is sent to one RF port of DP-MZM2, and the other RF port of DP-MZM2 is left with no input.

First, the interference RF signal B is set as a pure microwave signal with a carrier frequency of 18 GHz to demonstrate the single frequency SIC. Figure 3 shows the optical spectra of the signal from DP-MZM1, which is monitored by an optical spectrum analyzer (Yokogawa AQ6370D) with 0.02 nm resolution bandwidth. The desired RF signal A is disconnected from the system. As can be seen from Fig. 3, when the SIC is disabled, the interference RF signal generates two optical sidebands after CS-DSB modulation in one sub-MZM in DP-MZM1. When the SIC is enabled, the two optical sidebands are deeply suppressed with about 35-dB suppression ratio, which means the interference RF signal B is suppressed.

To show the SIC performance of the system, an optical carrier from DP-MZM2 without modulation is combined with the optical signal from DP-MZM1. After photodetection at the PD, interference RF signals with and without SIC are generated and measured by a spectrum analyzer (R&S, FSWP-50), shown in Fig. 4. As can be seen from Fig. 4, cancellation of the interference RF signals with a cancellation depth around 58 dB is achieved. The RF cancellation depth is higher than the optical sideband suppression ratio shown in Fig. 3, because more

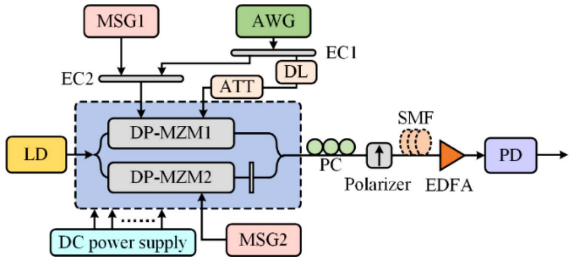

Fig. 2. Experimental setup of the proposed system. MSG, microwave signal source; AWG, arbitrary waveform generator; ATT, electrical attenuator; DL, electrical delay line; SMF, single-mode fiber.

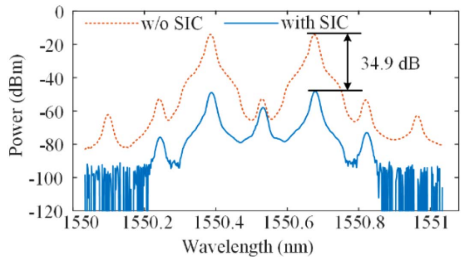

Fig. 3. Optical spectra of the signal from DP-MZM1 with and without SIC.

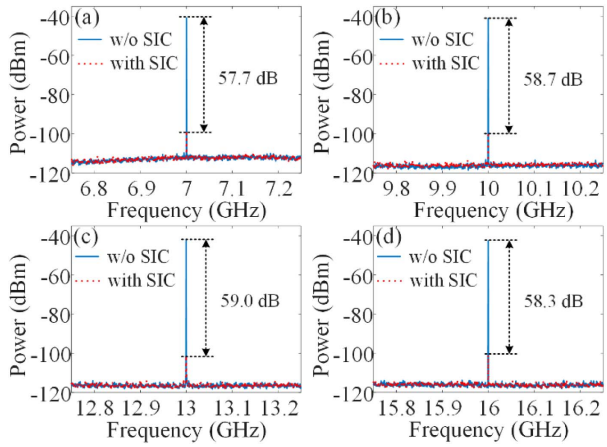

Fig. 4. Electrical spectra of the single frequency signal with and without SIC when the carrier frequency is (a) 7 GHz, (b) 10 GHz, (c) 13 GHz, and (d) 16 GHz.

precise parameter adjustment is adopted. Actually, in the process of parameter adjustment, ultrasmall time delay or amplitude mismatch of the interference RF signals will lead to very large cancellation depth change when the cancellation depth is higher than 35 dB, which means the stability of the system is the key issue to realize and maintain high cancellation depth.

Then, the LO signal and the desired RF signal A are applied to the modulator to verify the wideband SIC performance. To have a better observation of the wideband SIC, the desired RF signal is selected as a pure microwave signal, and the interference RF signal is a QPSK modulated signal with a data rate of 200 Mbps. In the experiment, the frequency of the received signal is set to 7 and 16 GHz, whereas the frequency of the LO signal is set to 1 GHz lower than that of the received RF signal. Figure 5 shows the electrical spectra of the donwconverted 1-GHz IF signals with and without the wideband interference cancellation. When the SIC is disabled, the desired IF signals at 1 GHz are overlapped with the wideband interference signals from about 0.9 to 1.1 GHz. In contrast, when the SIC is enabled, the wideband interferences are cancelled with cancellation depths of 27.3 and 25.7 dB, respectively, whereas the desired IF signals at 1 GHz do not have significant power degradation.

The downconversion from the RF band to the IF band is one possible approach to overcome fiber dispersion induced power fading of the desired signal. Figure 6(a) shows the theoretical curves of the power fading effect for the DSB modulated

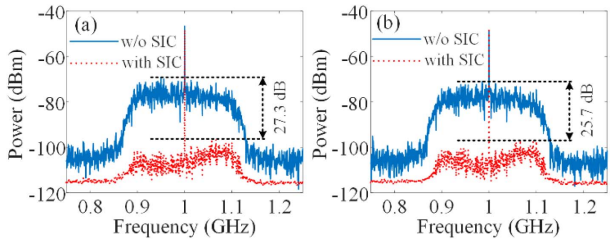

Fig. 5. Electrical spectra of the donwconverted IF signal with and without the wideband interference cancellation when the carrier frequency of the RF signal is (a) 7 GHz and (b) 16 GHz.

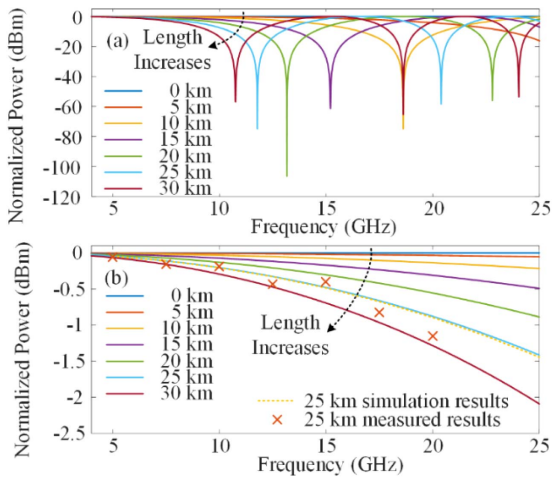

Fig. 6. Fading effect for (a) the DSB modulated RF signal and (b) the downconverted IF signal versus the frequency of the carrier.

signals with different RF frequencies and fiber lengths. Severe power fading effects are noticed, especially at some specific frequencies for each fiber length. Figure 6(b) shows the theoretical power fading for the uplink signals, which are downconverted to 1-GHz IF signals using corresponding LO signals, with different RF frequencies and fiber lengths. Although the fading effect is also more serious when the length of the fiber is increased, the magnitude of the signal fading is significantly reduced compared with the results shown in Fig. 6(a). If the frequency of the IF signal is further decreased, the fading effect can be better overcome. The dotted line in Fig. 6(b) shows the simulation results when the fiber length is 25 km, whereas the crosses in Fig. 6(b) show the corresponding experimental results, which are consistent with the theoretical and simulated curves. The measured data is processed by removing the influence of fiber attenuation and system responsivity on the results; thus only the power variation caused by fiber dispersion is reflected in the figure. In the calculation and simulation, the speed of light is 2.9979×10^8 m/s, the central wavelength is 1550.55 nm, and the dispersion coefficient of the fiber is 18 ps/ns/km.

In the experiment, the time delay and the attenuation are correspondingly tuned when the frequency of the applied microwave signal is changed, because of the nonuniform phase and amplitude response over such wide bandwidth. The performance of the proposed RF SIC system is much related to the stability of the system, including the stability of the bias points of the modulator and the time and power consistencies of the signals applied to DP-MZM1. In real-world applications, it is highly desired that bias control circuits for the bias points and adaptive control circuits for the time and power consistencies are employed, so that the stability and performance of the system can be increased.

In summary, a photonic approach for simultaneous wideband RF SIC and frequency downconversion in in-band full-duplex ROF systems is proposed and experimentally demonstrated for the first time, to the best of our knowledge. The key contribution of the work is that it combines the concept of SIC and IF transmission in ROF systems mainly in a single DP-QPSK modulator. The proposed approach can greatly reduce the cost of the in-band full-duplex ROF systems because the two main issues faced in the in-band full-duplex ROF system, namely, self-interference and dispersion induced distortion, are simultaneously handled: the self-interference is cancelled directly in the optical domain in the base station so that the fiber transmission will not cause the interference to reappear, whereas the fiber dispersion induced fading effect is overcome by employing IF transmission between the base station and the central office. An experiment is carried out. SIC in a wide frequency range is demonstrated both in single frequency and in wideband. The cancellation depth for single frequency SIC can be 58 dB, whereas that for the wideband SIC is larger than 25 dB. The fading effect of the proposed IF transmission system is also evaluated with a much better dispersion tolerance compared with the traditional RF transmission system.

Funding. National Natural Science Foundation of China (NSFC) (61601297, 61422108); Open Fund of IPOC (BUPT); Fundamental Research Funds for Central Universities.

REFERENCES

1. A. Stöhr, A. Akrout, R. Buß, B. Charbonnier, F. Dijk, A. Enard, S. Fedderwitz, D. Jäger, M. Huchard, F. Lecoche, J. Marti, R. Sambaraju, A. Steffan, A. Umbach, and M. Weiß, J. Opt. Netw. **8**, 471 (2009).
2. Y. Dong, H. Yüksel, and A. Molnar, IEEE J. Solid-State Circuits **50**, 1189 (2015).
3. M. Duarte, C. Dick, and A. Sabharwal, IEEE Trans. Wireless Commun. **11**, 4296 (2012).
4. S. Hong, J. Brand, J. Choi, and M. Jain, IEEE Commun. Mag. **52**(2), 114 (2014).
5. J. Yao, J. Lightwave Technol. **27**, 314 (2009).
6. J. Suarez, K. Kravtsov, and P. Prucnal, IEEE J. Quantum Electron. **45**, 402 (2009).
7. J. Suarez and P. Prucnal, IEEE Microw. Wireless Compon. Lett. **21**, 507 (2011).
8. M. Change, M. Fok, A. Hofmaier, and P. Prucnal, IEEE Microw. Wireless Compon. Lett. **23**, 99 (2013).
9. Q. Zhou, H. Feng, G. Scott, and M. Fok, Opt. Lett. **39**, 6537 (2014).
10. W. Zhou, P. Xiang, Z. Niu, M. Wang, and S. Pan, IEEE Photon. Technol. Lett. **28**, 849 (2016).
11. Y. Zhang, S. Xiao, H. Feng, L. Zhang, Z. Zhou, and W. Hu, Opt. Express **23**, 33205 (2015).
12. X. Han, B. Huo, Y. Shao, and M. Zhao, IEEE Photon. J. **9**, 5501308 (2017).
13. Y. Chen, A. Wen, L. Shang, and Y. Wang, Opt. Laser Technol. **43**, 1167 (2011).